Coherent high- and low-latitude control of the northwest African hydrological balance

RIK TJALLINGII[1]*†, MARTIN CLAUSSEN[2,3]†, JAN-BEREND W. STUUT[1], JENS FOHLMEISTER[4], ALEXANDRA JAHN[5], TORSTEN BICKERT[1], FRANK LAMY[6] AND URSULA RÖHL[1]

[1]MARUM - Center for Marine Environmental Sciences, University of Bremen, Leobener Straße, D-28359 Bremen, Germany
[2]Max Planck Institute for Meteorology, D-20146 Hamburg, Germany
[3]Meterological Institute, University of Hamburg, D-20146 Hamburg, Germany
[4]Heidelberg Academy of Science, D-69120 Heidelberg, Germany
[5]Department of Atmospheric and Oceanic Sciences, McGill University, H3A2K6 Montreal, Québec, Canada
[6]Alfred Wegener Institute für Polar and Marine Research, D-27570 Bremerhaven, Germany
*Present address: Institute for Geosciences, University of Kiel, D-24118 Kiel, Germany
†e-mail: rtj@gpi.uni-kiel.de; martin.claussen@zmaw.de

Published online: 7 September 2008; corrected online: 18 September 2008; doi:10.1038/ngeo289

The evolution of the northwest African hydrological balance throughout the Pleistocene epoch influenced the migration of prehistoric humans[1]. The hydrological balance is also thought to be important to global teleconnection mechanisms during Dansgaard–Oeschger and Heinrich events[2]. However, most high-resolution African climate records do not span the millennial-scale climate changes of the last glacial–interglacial cycle[1,3–5], or lack an accurate chronology[6]. Here, we use grain-size analyses of siliciclastic marine sediments from off the coast of Mauritania to reconstruct changes in northwest African humidity over the past 120,000 years. We compare this reconstruction to simulations of palaeo-humidity from a coupled atmosphere–ocean–vegetation model. These records are in good agreement, and indicate the reoccurrence of precession-forced humid periods during the last interglacial period similar to the Holocene African Humid Period. We suggest that millennial-scale arid events are associated with a reduction of the North Atlantic meridional overturning circulation and that millennial-scale humid events are linked to a regional increase of winter rainfall over the coastal regions of northwest Africa.

Long-term humidity variations in tropical and subtropical regions influenced by the African monsoon are related to precession-forced changes in low-latitude summer insolation[7–9]. In the Sahara and Sahel regions, orbital-forced variation of the monsoonal strength resulted in extreme environmental variations from extensive annual grasslands with numerous lakes during the early Holocene African Humid Period (AHP), to the present-day arid desert conditions[3,5,9,10]. Despite the rather gradual orbital-scale forcing, model studies suggest that nonlinear biogeophysical feedbacks between precipitation and vegetation cover might cause an abrupt transition from a largely vegetated Sahara to a hyper-arid Sahara desert, such as the termination of the AHP around ~5.5 kyr BP (refs 9,11–13). On the other hand, abrupt millennial-scale dry events that co-occur with cold North Atlantic sea surface temperatures (SSTs) during Heinrich ice surge events have been explained by a southward migration of the intertropical convergence zone (ITCZ) and its associated rainfall belt[3,4,6,14,15]. Therefore, northwest Africa is a key location to study the interaction between low-latitude African monsoon systems and high-latitude millennial-scale climate change.

Marine sediment core GeoB7920 (20° 45, 09′ N–18° 34, 90′ W, 2,278 m water depth) is ideally situated to record variations of the northwest African hydrological balance and vegetation cover owing to its position directly under the major African dust track[5,16] (Fig. 1). Off northwest Africa, aeolian-transported dust can be distinguished by the grain-size distribution of the siliciclastic fraction in marine sediments[16–19]. Although grain-size variations of aeolian-transported dust have been explained by changes in wind strength, transport distance and source area[16–18], variations of the total aeolian dust contribution are predominantly related to the continental vegetation cover and subsequent subaerial erosion[5,17] (see Supplementary Information). We measured the grain-size distribution of the siliciclastic sediment fraction of GeoB7920-2, and expressed these as proportions of three statistically relevant endmembers by endmember modelling[20] (see Supplementary Information). On the basis of the regional distribution of endmembers retrieved from surface sediments of the northwest African margin[19], the three endmembers of core GeoB7920-2 are interpreted as coarse aeolian dust (EM1), fine aeolian dust (EM2) and hemi-pelagic mud (EM3) that can be related to fluvial transport (see Supplementary Information). The proportions of aeolian endmembers EM1 and EM2 are related to the subaerial erosion and subsequently to the continental vegetation cover[5,17], whereas the proportions of EM3 are rather a measure of river runoff[19] (see Supplementary Information). We use the log ratio of the non-aeolian endmember EM3, and the aeolian endmembers EM1 and EM2 ($\log[EM3/(EM1 + EM2)]$) to indicate relative changes of the continental humidity and vegetation cover. In addition, the $\delta^{13}C$ record of the benthic foraminifera *Cibicidoides wuellerstorfi* is used to indicate changes of the deep-water ventilation and the North Atlantic meridional overturning[21].

Low contributions of the aeolian endmembers EM1 and EM2 and high contributions of fluvial end member EM3 indicate highly positive humidity values (Fig. 2e). Pronounced humid periods occur during periods of maximum low-latitude summer insolation during Marine Isotope Stage (MIS) 5 and the early Holocene

© 2008 Macmillan Publishers Limited. All rights reserved.

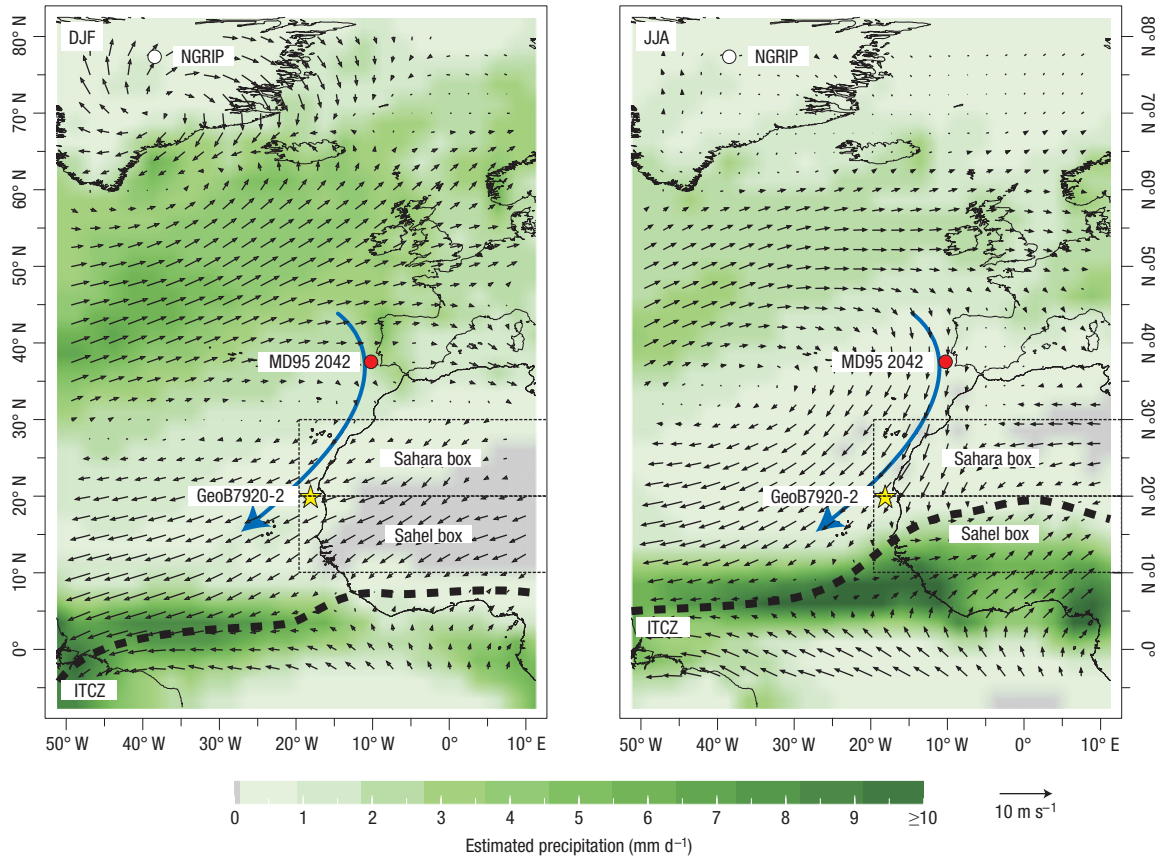

Figure 1 Average precipitation rates, surface wind direction and strength over the northeastern Atlantic for boreal winter and summer. The map shows the position of sediment core GeoB7920-2 (yellow star) and MD95 2042 (red circle), the North Greenland Ice core Project (NGRIP) ice core (white circle) and the two grid boxes of the CLIMBER-2 model used in this study. The North Atlantic eastern boundary current (blue arrow) and the position of the ITCZ (black dotted line) are indicated as well. The average precipitation rates, surface wind direction and strength are calculated for the period 1984–2003 by the International Research Institute for Climatic Prediction (http://iri.ldeo.colombia.edu).

epoch (Fig. 2). The strongly enhanced humidity occurring during the early Holocene coincides with the AHP, during which the Sahara was largely covered by grasslands[3,5,10,12]. Humid conditions similar to the AHP occur during MIS5a and MIS5c and indicate reoccurrence of AHPs (Fig. 2). Continuously arid conditions occur during the maximum glacial conditions of MIS4 and MIS2, whereas MIS3 is characterized by abrupt millennial-scale alternations of arid and humid events (Fig. 2). Millennial-scale dry events coincide with abrupt decreases in Greenland air temperatures (Fig. 2a) and eastern boundary current SSTs (Fig. 2b), and lower benthic $\delta^{13}C$ values of GeoB7920-2 (Fig. 2d), all of which indicate strongly reduced North Atlantic meridional overturning[21]. These dry events can be related to Greenland stadial events 25, 24, 22, 21 and 20 of MIS5, and Heinrich events H6, H5, H4 and H1 and the Younger Dryas (Fig. 2), which have been related to North Atlantic freshwater pulses[5,22,23]. Dry events associated with H3 and H2 occur during conditions of stronger glaciation and are less well expressed or even absent in the humidity record (Fig. 2e), but clearly visible in the $\delta^{13}C$ record of GeoB7920-2 (Fig. 2d). The millennial-scale humid events of MIS3 occur during relatively mild Northern Hemisphere interstadial conditions and seem to be independent of low-latitude insolation variations (Fig. 2).

Two model simulations were analysed to investigate the response of the North African precipitation and vegetation cover to low-latitude insolation variations and high-latitude Heinrich events. The simulations were carried out with the CLIMBER-2 model, which is a global atmosphere–ocean–vegetation (AOV) model of intermediate complexity (see Supplementary Information). The rather coarse geographic resolution of CLIMBER-2 covers northern Africa by three grid boxes corresponding to the Sahara, the Sahel and tropical northern Africa. As marine sediment core GeoB7920 is located at the border of the Saharan and Sahelian grid box (Fig. 1), climate and vegetation changes will be considered in both of these grid boxes.

The AOV-IC simulation describes the long-term climate variations over multiple precessional cycles by using external forcing of orbital-induced insolation, prescribed variations in atmospheric CO_2 concentrations and prescribed inland ice variations derived from global sea level variations[24]. The AOV-IC-f simulation describes millennial-scale climate variations between 60 and 20 kyr BP. In contrast to AOV-IC, AOV-IC-f includes an additional freshwater forcing in the North Atlantic to simulate Heinrich events (triggered every 7.5 kyr) and Dansgaard–Oeschger events[25] (see Supplementary Information). As the timing of these simulated Heinrich events was prescribed, but not predicted, these events are not synchronous with real Heinrich events. Moreover, owing to the geographic coarseness of CLIMBER-2, these simulations are considered more a test of concept rather than a detailed prediction.

© 2008 Macmillan Publishers Limited. All rights reserved.

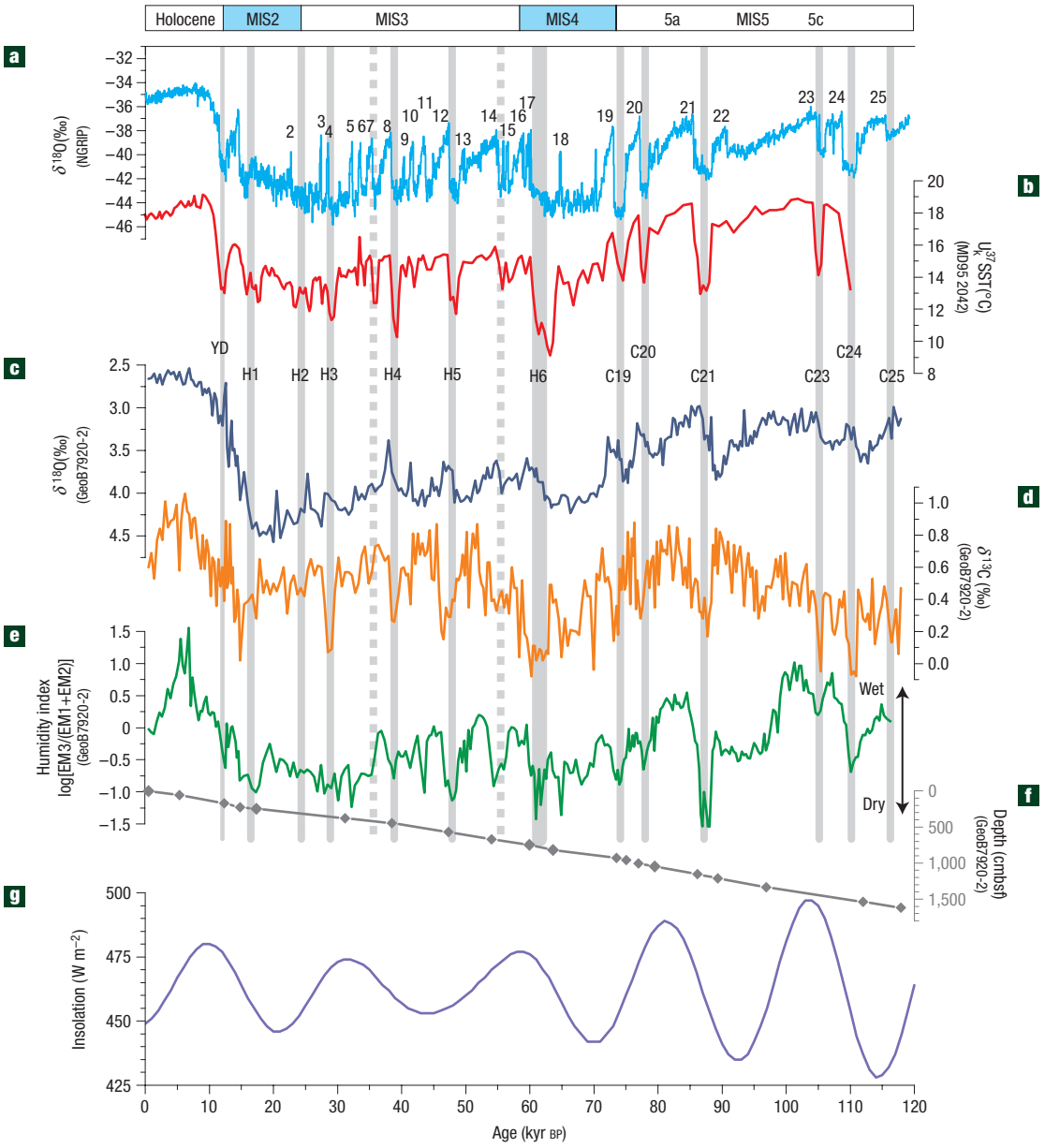

Figure 2 Palaeoenvironmental records of the NGRIP ice core, MD95 2042 and GeoB7920 for the last 120 kyr BP. a, Variations of the air temperature over Greenland indicated by the $\delta^{18}O$ record of the NGRIP ice core and the numbered interstadial events[30]. **b**, Alkenone-based SST reconstruction of core MD95 2042 (ref. 23). **c**,**d**, $\delta^{18}O$ (**c**) and $\delta^{13}C$ (**d**) record of benthic foraminifera *Cibicidoides wuellerstorfi* of core GeoB7920-2. **e**, Continental humidity index of core GeoB7920-2 as indicated by log[EM3/(EM1+EM2)]. **f**, Age–depth relationship of GeoB7920-2 (see Supplementary Information). **g**, Average summer insolation at 30° N. The grey bars indicate North Atlantic ice rafted debris events[22,23].

The AOV-IC simulation of the precipitation shows dominantly precession-forced variations in both the Saharan and the Sahel regions (Fig. 3a,b), which are related to an increase of the monsoonal strength and a northward migration of the ITCZ during precession maxima[9,11]. In the Sahara region, these precession-forced variations are accompanied by a large-scale and, relative to orbital forcing, abrupt northward expansion of the Saharan grassland (Fig. 3a) due to nonlinear biogeophysical feedback[9,11,12] (see Supplementary Information). These precession-forced humid periods corroborate the humid periods during MIS5 and the Holocene in core GeoB7920 (Fig. 3). Both the AOV-IC simulation and the proxy data indicate that the expansion and retreat of Saharan vegetation occurs much faster than changes in orbital forcing, which is in agreement with what was found for the Holocene AHP (refs 5,8). Hence, all humid periods can be considered as a test of the nonlinear climate and vegetation response. During the last glacial period, pronounced precession-forced humid periods are absent in the AOV-IC simulation of the Sahara (Fig. 3a). Expansion of the Northern Hemisphere ice caps in combination with weaker precessional forcing during the last glacial prevented the African monsoonal system from influencing the Sahara, creating a colder

© 2008 Macmillan Publishers Limited. All rights reserved.

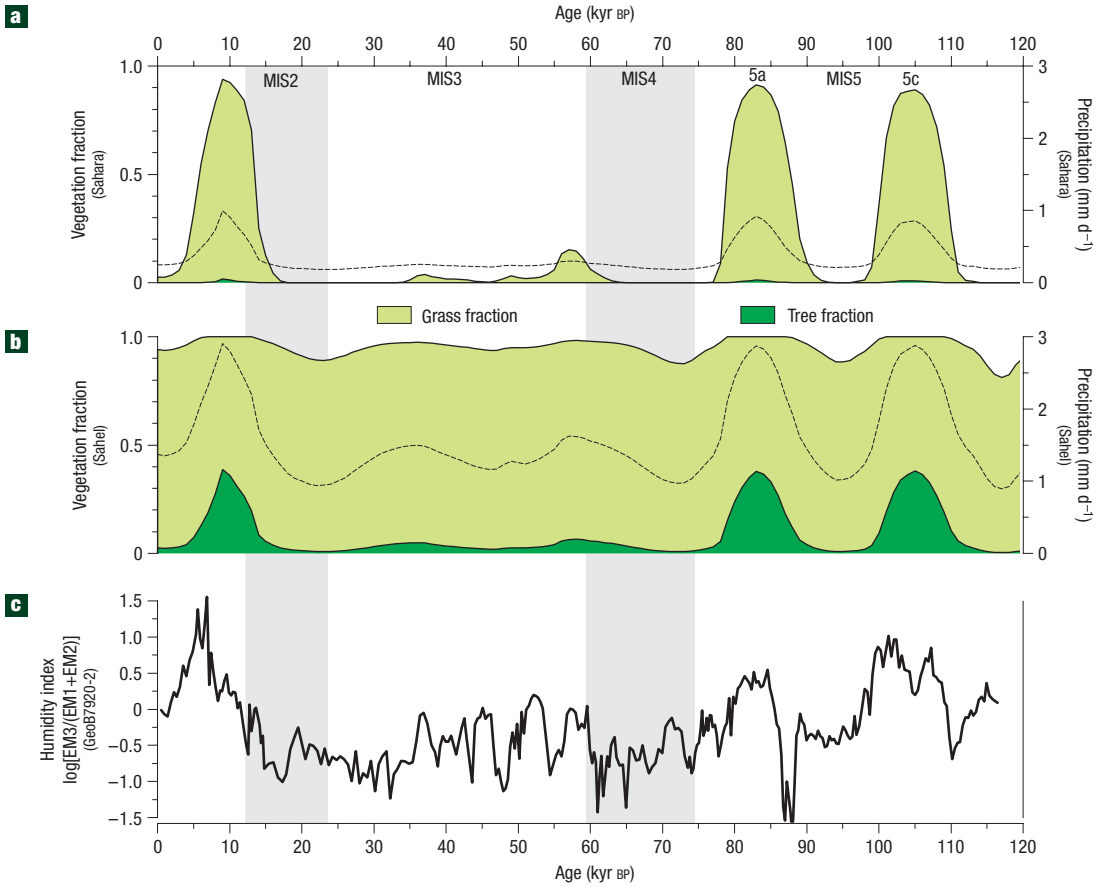

Figure 3 Model–data comparison of the northern Africa humidity and vegetation cover during the last 120 kyr BP. a,**b**, AOV-IC model simulation of the vegetation cover and the annual mean daily precipitation (mm d^{-1}) (black dashed line) in the Sahara grid box (20°–30° N) (**a**) and the Sahel grid box (10°–20° N) (**b**). **c**, Temporal variation of the continental humidity index of core GeoB7920.

and drier climate. In the humidity record of GeoB7920, similar dry conditions are shown only during the maximum glacial conditions of MIS4 and MIS2 (Fig. 3).

Both the proxy data and the AOV-IC-f simulation (Fig. 4) indicate millennial-scale dry events in response to freshwater pulses in the North Atlantic. Although the Heinrich event-like freshwater perturbations of the AOV-IC-f simulation were prescribed every 7.5 kyr, the corresponding dry events in the Sahel region are strikingly similar to the dry events seen during H6, H5 and H1, and to a lesser extent H4 and H3 in the humidity record of GeoB 7920-2 (Fig. 4). This suggests that millennial-scale dry events in GeoB 7920-2 can be interpreted as a response to freshwater pulses into the North Atlantic. The abrupt millennial-scale humid events during MIS3 indicated in GeoB7920 (Fig. 3c) do not occur in the AOV-IC nor the AOV-IC-f simulation.

Proxy data and the model simulations indicate that orbital-forced strengthening of the African monsoon during MIS5 resulted in an expansion of the Saharan vegetation cover comparable to the Holocene AHP. These long-term variations are in agreement with the tropical western African hydrological balance, which seemingly depends on moisture transport from the eastern equatorial Atlantic[7,8]. In the modelling simulations, moisture transport from the tropical and subtropical Atlantic is the dominant process. However, North African pollen and plant macrofossil data[10] and the aeolian dust record in the northern Red Sea region[25] suggest that moisture transport from the North Atlantic and Mediterranean Sea into Africa's Mediterranean regions cannot be neglected. Unfortunately, the extent to which moisture transport from the Mediterranean affects North African climate cannot be assessed by the CLIMBER-2 simulations.

Proxy data and the AOV-IC-f simulation convincingly show that the millennial-scale dry events on the northern African continent are forced by high-latitude Heinrich events, which supports the results of previous studies[3,4,6,14,15]. However, generally dry conditions over the North African continent during periods of stronger glaciation probably resulted in a weaker expression of H3 and H4, and the absence of H2 in the humidity record of GeoB7620-2. In the model, the Heinrich event forcing is transmitted through large-scale changes in the North Atlantic overturning circulation[26] (see Supplementary Information), which is supported by the $\delta^{13}C$ record of GeoB7920-2 (Fig. 2d). Alternatively, transmission of cold North Atlantic SST to lower latitudes by the eastern boundary current has been suggested[4,6,15,22,23]. Nevertheless, the millennial-scale dry events in both the proxy data and the model simulation strongly suggest a decoupling of northern high-latitude millennial-scale climate change and the precessional-forced low-latitude African monsoon, which supports humidity reconstructions of the northwest African subtropics[3,4,14,15]. However, regarding the differences between West African tropical humidity records[8,14], there seems to be no consensus on the occurrence of millennial-scale climate variations in the African tropics. This might be related to

© 2008 Macmillan Publishers Limited. All rights reserved.

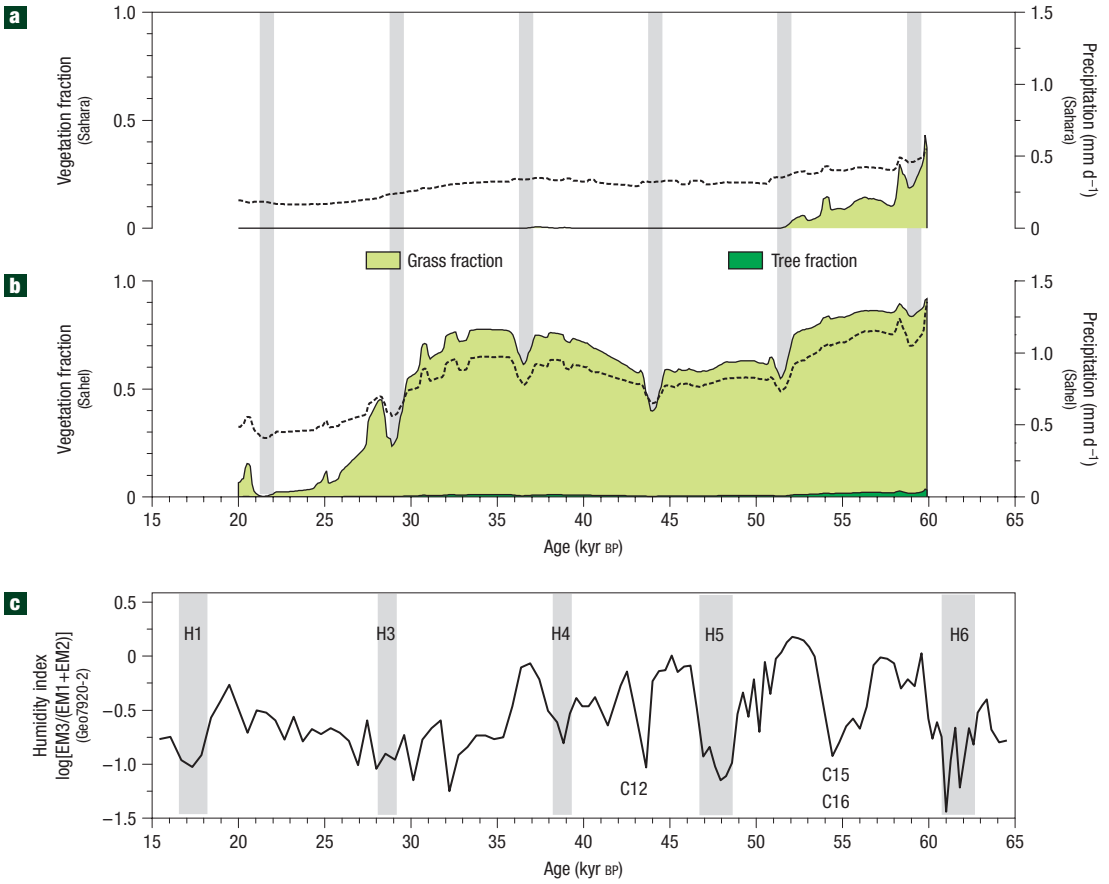

Figure 4 Model–data comparison of the northern Africa humidity and vegetation cover from 65 to 15 kyr BP. a,**b**, AOV-IV-f model simulation of the vegetation cover and the annual mean daily precipitation (mm d^{-1}) (black dashed line) in the Sahara grid box (20°–30° N) (**a**) and the Sahel grid box (10°–20° N) (**b**). The grey bars indicate North Atlantic freshwater pulses triggered every 7.5 kyr. **c**, Temporal variation of the continental humidity index of core GeoB7920. The grey bars indicate North Atlantic ice rafted debris events[22,23].

the response of each distinct humidity proxy to different regional influences.

The millennial-scale humid events shown in the humidity record of GeoB7920-2 during MIS3 are remarkably similar to millennial-scale humid events recorded in the western Mediterranean[27–29]. These humid events have been explained by a southward movement of the mid-latitude wind systems and an increased influence of North Atlantic winter precipitation[27–29]. Although the coarse scale of the CLIMBER-2 model does not reproduce these humid events in the AOV-IC-f simulation, such a scenario is in agreement with and further supports a decoupling of northern high-latitude millennial-scale climate change and the low-latitude African monsoon during MIS3 (refs 3,4,8,14).

To summarize, here we present for the first time proxy data and model simulations that consistently reveal vegetation and climate change due to climatic precession in the North African subtropical regions during the last glacial–interglacial cycle. The model prediction of a largely vegetated Sahara, as well as an abrupt expansion and retreat of Saharan grassland vegetation during isotope stages 5a and 5c, is corroborated by proxy data. Moreover, model and proxy data indicate that high-latitude Heinrich events cause millennial-scale dry spells in North Africa. However, the millennial-scale humid events indicated in GeoB7920-2 during MIS3 cannot be assessed by the CLIMBER-2 simulations. High-resolution model simulations are required to assess the geographical extent of dry events in North Africa, the role of the eastern boundary current and the influence of winter precipitation on North African climate and vegetation dynamics.

METHODS

The siliciclastic sediment fraction was isolated by dissolving carbonate, organic matter and biogenic opal from ~0.5 ml bulk sediment in HCl, H_2O_2 and NaOH respectively. Random microscope observations were carried out to confirm the removal of all biogenic constituents. Each sample was briefly heated with about 300 mg of $Na_4P_2O_7{\cdot}10H_2O$ directly before measuring to avoid the formation of aggregates in the fine-grained fraction. The grain-size distribution of each sample ($N = 315$) was analysed with a Coulter LS200 laser particle sizer that measures particles in the range of 0.4–2,000 μm in 92 size classes.

The endmember modelling algorithm[20] approximates a theoretical grain-size distribution from the total set of grain-size measurements ($N = 315$). The model estimates the minimum number of endmembers required for a satisfactory approximation of the data (see Supplementary Information). The measured grain-size distributions of core GeoB7920 can now be expressed as relative proportions of the constant-sum of the three endmembers ($EM1 + EM2 + EM3 = 1$).

Stable isotope analysis ($\delta^{13}C$ and $\delta^{18}O$) measurements were recorded on the benthic foraminifera *Cibicidoides wuellerstorfi* (>250 μm) every 5 cm ($N = 322$). Analyses were carried out on a Finnigan MAT 252 micro-mass spectrometer coupled to an automated carbonate preparation device. The precision of this system is within 0.05‰ and 0.07‰ (Vienna PeeDee Belemnite) with respect to an internal standard for $\delta^{13}C$ and $\delta^{18}O$, respectively.

© 2008 Macmillan Publishers Limited. All rights reserved.

The model simulations were carried out with the global AOV CLIMBER-2 model of intermediate complexity for the period 120–0 kyr BP (AOV-IC) and 60–20 kyr BP (AOV-IC-f). Details on the simulations are given in the Supplementary Information.

Received 7 November 2007; accepted 31 July 2008; published 7 September 2008.

References

1. Kuper, R. & Kröpelin, S. Climate-controlled Holocene occupation in the Sahara: Motor of Africa's evolution. *Science* **313**, 803–807 (2006).
2. Broecker, W. S. Does the trigger for abrupt climate change reside in the ocean or in the atmosphere? *Science* **300**, 1519–1522 (2003).
3. Gasse, F. Hydrological changes in the African tropics since the Last Glacial Maximum. *Quat. Sci. Rev.* **19**, 189–211 (2000).
4. Street-Perrott, F. A. & Perrott, R. A. Abrupt climate fluctuations in the tropics: the influence of Atlantic Ocean circulation. *Nature* **343**, 607–612 (1990).
5. deMenocal, P. B. *et al.* Abrupt onset and termination of the African Humid period: Rapid climate response to gradual insolation forcing. *Quat. Sci. Rev.* **19**, 347–361 (2000).
6. Zhao, M., Mercer, J. L., Eglinton, G., Higginson, M. J. & Huang, C.-Y. Comparative molecular biomarker assessment of phytoplankton paleoproductivity for the last 160 kyr off Cap Blanc, NW Africa. *Org. Geochem.* **37**, 72–97 (2006).
7. Schefuß, E., Schouten, S., Jansen, J. H. F. & Sinninghe Damsté, J. S. African vegetation controlled by tropical sea surface temperatures in the mid-Pleistocene period. *Nature* **422**, 418–421 (2003).
8. Weldeab, S., Lea, D. W., Schneider, R. R. & Andersen, N. 155,000 Years of West African Monsoon and Ocean thermal evolution. *Science* **316**, 1303–1307 (2007).
9. Claussen, M. *et al.* Simulation of an abrupt change in Saharan vegetation in the mid-Holocene. *Geophys. Res. Lett.* **26**, 2037–2040 (1999).
10. Jolly, D., Harrison, S. P., Damnati, B. & Bonnefille, R. Simulated climate and biomes of Africa during the late quaternary: Comparison with pollen and lake status data. *Quat. Sci. Rev.* **17**, 629–657 (1998).
11. Renssen, H., Brovkin, V., Fichefet, T. & Goosse, H. Simulation of the Holocene climate evolution in Northern Africa: The termination of the African Humid Period. *Quat. Int.* **150**, 95–102 (2006).
12. Liu, Z. *et al.* Simulating the transient evolution and abrupt change of Northern Africa atmosphere-ocean-terrestrial ecosystem in the Holocene. *Quat. Sci. Rev.* **26**, 1818–1837 (2007).
13. Liu, Z., Wang, Y., Gallimore, R., Notaro, M. & Prentice, I. C. On the cause of abrupt vegetation collapse in North Africa during the Holocene: Climate variability vs. vegetation feedback. *Geophys. Res. Lett.* **33**, L22709 (2006).
14. Adegbie, A. T., Schneider, R. R., Rohl, U. & Wefer, G. Glacial millennial-scale fluctuations in central African precipitation recorded in terrigenous sediment supply and freshwater signals offshore Cameroon. *Palaeogeogr. Palaeoclimatol. Palaeoecol.* **197**, 323–333 (2003).
15. deMenocal, P. B., Ortiz, J., Guilderson, T. & Sarnthein, M. Coherent high- and low-latitude climate variability during the Holocene Warm Period. *Science* **288**, 2198–2202 (2000).
16. Sarnthein, M., Tetzlaff, G., Koopmann, B., Wolter, K. & Pflaumann, U. Glacial and interglacial wind regimes over the eastern subtropical Atlantic and North-West Africa. *Nature* **293**, 193–196 (1981).
17. Parkin, D. W. & Shackleton, N. J. Trade wind and temperature correlations down a deep-sea core off the Saharan coast. *Nature* **245**, 455–457 (1973).
18. Weltje, G. J. & Prins, M. A. Muddled or mixed? Inferring palaeoclimate from size distributions of deep-sea clastics. *Sedim. Geol.* **162**, 39–62 (2003).
19. Holz, C., Stuut, J. b. W. & Henrich, R. Terrigenous sedimentation processes along the continental margin off NW Africa: Implications from grain-size analysis of seabed sediments. *Sedimentology* **51**, 1145–1154 (2005).
20. Weltje, G. J. & Prins, M. A. Genetically meaningful decomposition of grain-size distributions. *Sedim. Geol.* **202**, 409–424 (2007).
21. Vidal, L. *et al.* Evidence for changes in the North Atlantic Deep Water linked to meltwater surges during the Heinrich events. *Earth Planet. Sci. Lett.* **146**, 13–27 (1997).
22. Chapman, M. R., N J, S. & Duplessy, J.-C. Sea surface temperature variability during the last glacial-interglacial cycle: Assessing the magnitude and pattern of climate change in the North Atlantic. *Palaeogeogr. Palaeoclimatol. Palaeoecol.* **157**, 1–25 (2000).
23. Bard, E. Abrupt climate changes over millennial timescales: Climate shock. *Phys. Today* **55**, 32–38 (2002).
24. Claussen, M., Fohlmeister, J., Ganopolski, A. & Brovkin, V. Vegetation dynamics amplifies precessional forcing. *Geophys. Res. Lett.* **33**, L09709 (2006).
25. Arz, H. W., Lamy, F., Pätzold, J., Müller, P. J. & Prins, M. Mediterranean moisture source for an early-Holocene humid period in the Northern Red Sea. *Science* **300**, 118–121 (2003).
26. Claussen, M., Ganopolski, A., Brovkin, V., Gerstengarbe, F. W. & Werner, P. Simulated global-scale response of the climate system to Dansgaard/Oeschger and Heinrich events. *Clim. Dyn.* **21**, 361–370 (2003).
27. Allen, J. R. M. *et al.* Rapid environmental changes in southern Europe during the last glacial period. *Nature* **400**, 740–743 (1999).
28. Combourieu Nebout, N. *et al.* Enhanced aridity and atmospheric high-pressure stability over the western Mediterranean during the North Atlantic cold events of the past 50 kyr. *Geology* **30**, 863–866 (2002).
29. Moreno, A. *et al.* Links between marine and atmospheric processes oscillating on a millennial time-scale. A multi-proxy study of the last 50,000 yr from the Alboran Sea (Western Mediterranean Sea). *Quat. Sci. Rev.* **24**, 1623–1636 (2005).
30. NGRIP-Members. High-resolution record of Northern Hemisphere climate extending into the last interglacial period. *Nature* **431**, 147–151 (2004).

Supplementary Information accompanies the paper at www.nature.com/naturegeoscience.

Acknowledgements

We thank the crew and participants of Meteor cruise M53/1. The authors acknowledge G. J. Weltje for providing the End-Member Model Algorithm and the constructive discussion with A. Ganopolski, E. Bauer, V. Brovkin, H. Arz and M. Prins. M. Segl is thanked for supervising the stable isotope analyses. This research was supported by the Deutsche Forschungsgemeinschaft as part of the DFG Research Center for Ocean Margins of the University of Bremen.

Author contributions

Experimental work, data analysis and interpretation of the proxy data were carried out by R.T., J.B.W.S., T.B., F.L. and U.R. The CLIMBER model simulations were set up and carried out by M.C., J.F. and A.J.

Author information

Reprints and permission information is available online at http://npg.nature.com/reprintsandpermissions. Correspondence and requests for materials should be addressed to R.T. or M.C.

© 2008 Macmillan Publishers Limited. All rights reserved.